

MODIS SEMI-ANNUAL REPORT: JAN/01/03 - JUN/30/03

Radiative Transfer Based Synergistic MODIS/MISR Algorithm for the Estimation of Global LAI & FPAR

(Contract: NAS5-96061)

N. V. Shabanov, W. Yang, B. Tan, H. Dong, Y. Knyazikhin, R. B. Myneni
Geography Department, Boston University, 675 Commonwealth Avenue, Boston, MA 02215

Summary of the algorithm. The objective of the contract is to develop a radiative transfer based synergistic algorithm for estimation of global leaf area index (LAI) and fraction of photosynthetically active radiation absorbed by vegetation (FPAR). The algorithm consists of a main procedure that exploits the spectral information content of MODIS measurements and the angular information content of MISR measurements to derive accurate estimation of LAI and FPAR. Should this main algorithm fail, a backup algorithm is triggered to estimate LAI and FPAR using vegetation indices. Both algorithms are capable of executing in MODIS-only or MISR-only mode, should cloud contamination, data frequency and spatial or temporal resolution requirements hinder a joint MODIS/MISR mode of operation. The MODIS-only mode of the algorithm requires a land cover classification that is compatible with the radiative transfer model used in the derivation. Such a classification is currently a part of MODIS landcover product and utilized in collection 4 MODIS LAI and FPAR algorithm. Therefore, our algorithm has interfaces with the MODIS/MISR surface reflectance product and the MODIS Land Cover Product. Validation of the LAI/FPAR product is an important part of algorithm development. We developed scaling-based validation strategy of the LAI and FPAR product and implementing it currently in our validation activity. Successful validation will be accomplished if timely and accurate product uncertainty information becomes routinely available to the product users within two years after Terra's launch.

Summary of work performed during the first half of 2003 (January through June):

- Assessment of the performance of the MODIS LAI algorithm as a function of input data uncertainties – case study for grasses;
- Analysis of the performance of the MODIS LAI and FPAR algorithm over broadleaf forests;
- Maintenance of the algorithm: a) patch delivery for the TERRA LAI and FPAR algorithms to fix problem of incorrectly reading negative View Azimuth Angles, b) patch delivery for the TERRA LAI and FPAR algorithms to fix problem of assigning a fill value (instead of LAI=0) to pixels located at the Northern high latitudes during winter time, c) report to the MODIS landcover team about errors in latest version (collection 3) of the 6-biome land cover product (MOD12Q1), input to the collection 4 MODIS AQUA and TERRA LAI & FPAR algorithms, d) patch delivery for AQUA LAI & FRAR algorithm to update AQUA LUT with the results of collection 4 science test for TERRA LAI and FPAR product;
- Development of the strategy for the future work and submission of the proposal in response to the NASA Research Announcement (NRA-03-OES-02), “Global Products of Leaf Area Index and Fraction Vegetation Absorbed PAR from the MODIS Sensors Onboard TERRA and AQUA: EOS Algorithm Refinement Proposal”;
- Talk at the Canadian Center for Remote Sensing, “Analysis of the performance of the MODIS LAI and FPAR Algorithm“, Ottawa, Ontario, Canada, May 26, 2003.

I. Assessment of the Performance of the MODIS LAI Algorithm as a Function of Input Data Uncertainties – Case Study for Grasses

Statement of the Problem

During validation of the collection 3 MODIS LAI and FPAR product it was found that MODIS LAI substantially overestimates field measured LAI. Field measurements of LAI collected over a 5 km by 5 km spatial area indicates mean LAI < 4. However MODIS LAI product averaged over the same area suggest LAI ~6. Research described below is aimed to resolve this inconsistency.

Data Used

- MOD15A2, 8-day LAI composite, collection 3, tile h10v05, composite 2001.185
- MODAGAGG, daily surface reflectance, collection 3, tile h10v05, days 185-192
- MOD12Q1, 6-biome classification map, at launch version, tile h10v05

Site Description

The MODIS LAI & FPAR product from the tile h10v05 was selected for this investigation. This tile contains the Konza Prairie Biological Station, Manhattan, KS, USA (located 39.0823° North and 96.56025° West; MODIS tile h10v05, line 110, sample 604). This site was selected for several recent major field campaigns within several projects: BigFoot (WWW 1), Flux Network (FLUXNET, WWW 2), Global Landcover Test Site Initiative (GLCTS, WWW 3), Long-Term Ecological Research (LTER, WWW 4). It is also an EOS core validation site (Privette et al., 1998; WWW 5), selected to provide a focus for satellite, aircraft, and ground data collection of land product validation. This site measures a number of ecological variables (leaf area index, biomass and NPP) besides carbon/water and energy fluxes, therefore provide a good opportunity to test MODIS LAI and FPAR products. MODIS data are being extracted regularly over these sites. We focus on analysis of the MODIS Collection 3 LAI product over the Konza site.

Impact of Biome Misclassification on LAI Retrievals

The assumption that vegetation within each pixel belongs to one of the six biomes impacts the MODIS LAI/FPAR retrievals. With misclassification, either main algorithm fails or it produces an incorrect LAI value (Tian et al., 2000; Myneni et al., 2002). Therefore we start our research with the analysis of the at-launch static LAI & FPAR Biome map used by the collection 3 LAI & FPAR algorithm.

Figure 1.1 shows distributions of biomes within the entire tile (1200km by 1200km) and areas of 100km by 100km and 20km by 20 km centered around the Konza validation site. According to the MODIS at-launch LAI & FPAR land cover map, biome 1 (Grasses and Cereal Crops) occupies 24% of the 5km by 5km area while the field measured value is 64% (Cohen et al., 2002). Therefore, more than $(64\%-24\%)/0.64=62.6\%$ of biome 1 pixels are misclassified, leading to the overestimation of the mean LAI value over the 5km by 5km (Figure 1.2a).

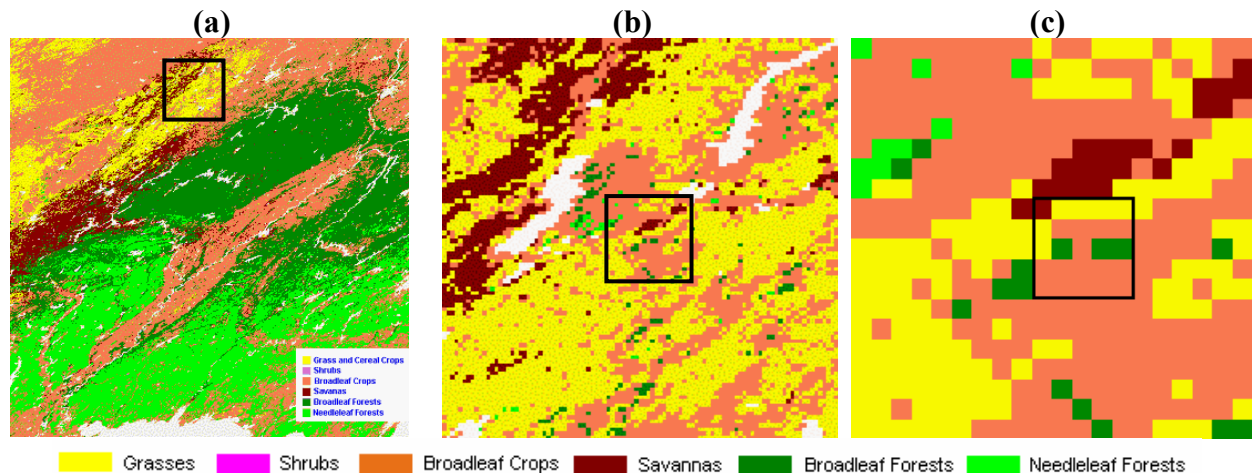


Figure 1.1: Spatial distribution of biomes over 1200km by 1200km (panel a), 100km by 100km (panel b), and 20km by 20 km (panel c) areas around the Konza validation site, as estimated by the at launch biome map. A 5km by 5km area where field measurements were performed is shown as a square in panel (c). According to this map, biome 1 (Grasses and Cereal Crops) occupies 24% of the 5km by 5km area while the field measured value is 64% (Cohen *et al.*, 2002). The at launch biome map identifies biome 3 (Broadleaf Crops) as the most probable biome type within the 5km by 5km area while field measurements show that only 0.3% of this area are occupied by Broadleaf Crops.

Does this example indicate that the global MODIS LAI field is incorrect?

The Collection 3 MOD15 LAI/FPAR algorithm uses the 1 km Surface Reflectance Product, 1 km at launch Land Cover Map to produce LAI and FPAR fields at 1 km resolution. Three random variables impact the retrievals. They are (a) uncertainties in surface reflectance product (e.g., due to correction for atmosphere and other environmental effects); (b) uncertainties in landcover identification (e.g., due to biome mixture within 1 km pixel), and (c) uncertainties in georegistration. The predicted LAI value in one pixel, therefore, should be treated as an observation of *a random variable* and thus an averaging over an extended homogeneous area is required to reduce variations due to uncertainties.

The size of an area is determined by the quality of algorithm input. This area should contain sufficient number of pixels with "good quality input." In the above example, 62.6% of biome 1 pixels located within the 5km by 5km area are attributed to incorrect biome types and thus this area cannot be taken as an area to examine variation in LAI values because the uncertainty in the biome map is too high. Figure 1.2a, therefore, is not indicative of the quality of the global product.

Grasses are majority biome in a larger, 100km by 100km area, making up 53% of the vegetated surface (Figures 2a and 3). Biome 1 pixels constitute several sufficient large homogeneous patches reducing uncertainties in the distribution of biomes. Figure 1.2b shows mean LAIs taken over biome 1 pixels in the entire tile and their standard deviations. One can see that, with a very

high probability, values of mean LAI do not exceed 4. Mean LAI derived from field measurements was 3.5

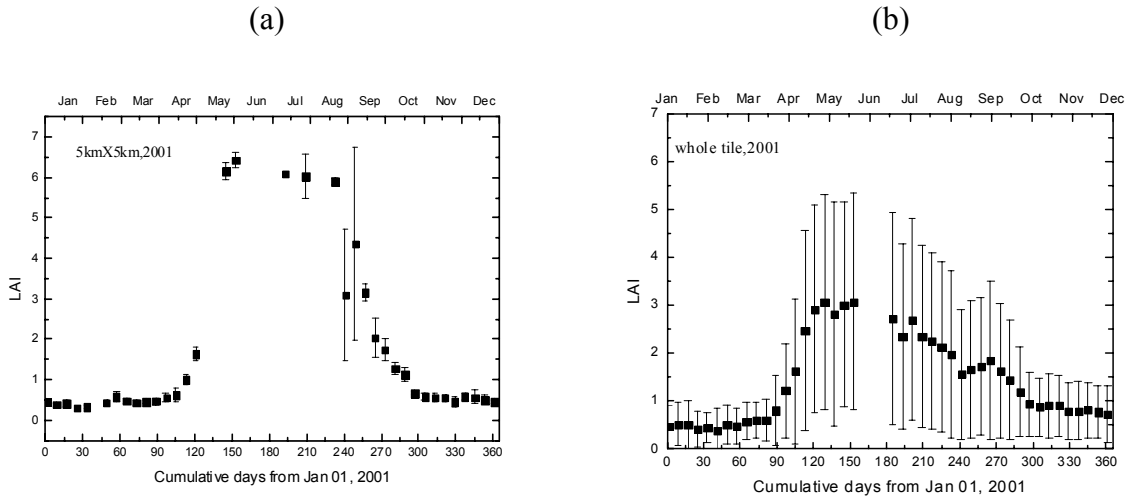


Figure 1.2: Temporal variation in mean LAI and standard deviation over a 5x5 grid centered around the tower (Panel a) and the entire tile (Panel b). The MODIS LAI product shows seasonality, as expected. However, mean LAI over the 5x5 grid are substantially overestimated: the MODIS algorithm predicts $LAI \approx 6$ while field measurements showed $LAI \leq 4$ for the same period. Mean LAI over the entire tile is about 4 which is close to that derived from the KONZA field campaign, July 11-17, 1999.

Impact of Uncertainties in Surface Reflectance on LAI Retrievals

In the MODIS LAI and FPAR algorithm, uncertainties in input surface reflectances set a limit to the quality of LAI retrievals. Generally, accuracy of the LAI and FPAR retrievals cannot be better than the overall accuracy in the input data. However, if the uncertainty information is properly used in the algorithm, the retrievals can be improved. In this study, provide an estimate of uncertainties in surface reflectance data and investigate their impact on the retrieval quality.

The analysis was performed with 8 days (July 4 through July 11, 2001) of the Collection 3 MODAGAGG surface reflectances at RED and NIR spectral channels for the tile h10v05. The following terminology is used in our study. “Valid pixel” is a pixel with Band_QC quality control at RED and NIR channels set to “Product produced at ideal quality” or “Product produced, less than ideal quality”. Otherwise the pixel is called “invalid pixel”. We separate two classes of surface reflectances. The first one termed “good quality surface reflectance” consists of biome 1 valid pixels for which at least 4 observations during 8 day period were available. The vegetation structure remains unchanged during the 8 day period and thus one should expect relative low variation in surface reflectances for this class. Invalid pixels for which 4 observations were available are attributed to the second class called “poor quality data.” Figure 1.4 shows histograms of relative variation in surface reflectances at RED and NIR spectral bands. Generally, variation in “good quality” data is 13% in RED band, 11% in NIR band. However, “poor quality data” exhibit high variations, about 70% and 13% for Red NIR bands,

respectively. One can conclude that Surface Reflectance Band QA convey correct information about quality of surface reflectance data.

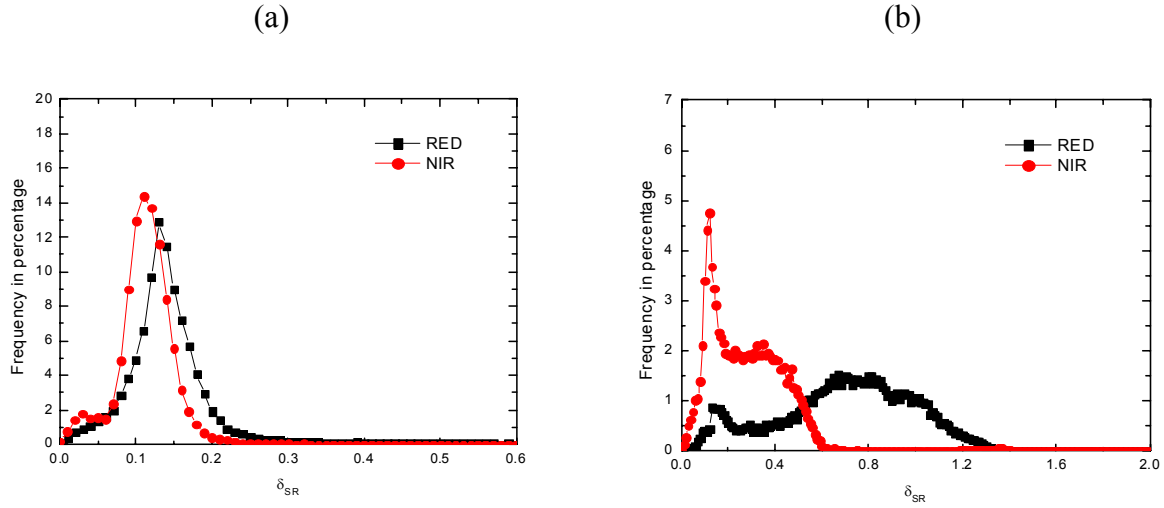


Figure 1.4: Histograms of the coefficient of variation of surface reflectances at RED and NIR spectral bands for “Good” (Panel a) “Poor” (Panel b) quality data. Note that a part of “poor” quality data exhibit low variation. This may indicate reliable data labeled as “poor quality”.

To identify factors that cause high variation in “poor quality” data, we decompose variation in the surface reflectance δ_{SR} as

$$\delta_{SR} = A \times \delta_{view} + B,$$

Here $A \times \delta_{view}$ is the variation in SR due to variations in view angle, and term B explains variation in SR due to other factors. Constants A and B can be determined from regression statistics, as shown in Figure 1.5. Their values were $A=0.3$ and $B=0.46$. When variation in view angles δ_{view} is close to 0, the variation in surface reflectance is about 46%. This suggests that variation in “poor quality” data are not caused by variation in the view angle.

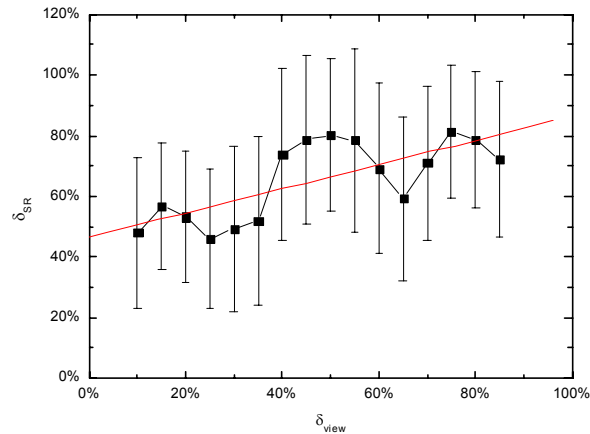


Figure 1.5: Regression line: δ_{SR} versus δ_{view} for “Poor Quality” .

The next step is to evaluate an impact of different input quality on LAI and FPAR retrievals. We used “valid data” and “invalid data” separately, as the input to the MODIS LAI/FPAR algorithm. The Retrieval Index (RI) defined as the ratio of pixels for which the main algorithm retrieved LAI and FPAR to the total number of processed pixels. The RI for “valid” and “invalid” data were 40% and 27%, respectively. This suggests that “valid data” is more likely to be retrieved by the main algorithm than “invalid data”. But there is no strong correlation between “valid data” and the RI (Figure 1.6).

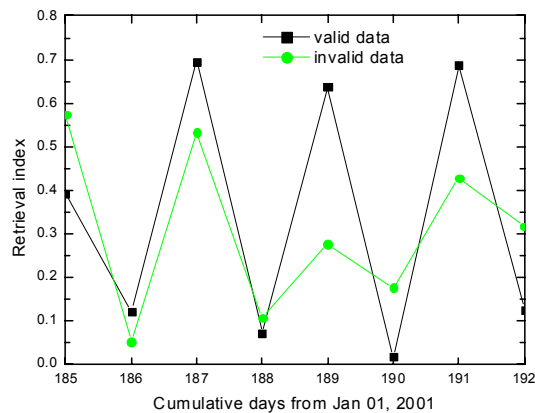


Figure 1.6: Daily variations of the Retrieval Index for “valid data” and “invalid data”

These results suggest that MODAGGAG QA itself is not sufficient to assure the successful execution of the LAI and FPAR algorithm. What are key factors that influence algorithm execution or failure? To address this question, surface reflectances are subdivided into the following subsets:

- **GL** (good quality, low uncertainties) – “good quality” data with relative uncertainties in surface reflectance less than 13%.

- **GH** (good quality, high uncertainties) - “good quality” data with relative uncertainties higher than 13%.
- **PL** (poor quality, low uncertainties) - “poor quality” data with relative uncertainties less than 13%.
- **PH** (poor quality, high uncertainties) - “poor quality” data for with relative uncertainties higher than 13%.

The RI for GL, GH, PL and PH data are 65%, 44%, 64% and 22%, respectively. The differences between RIs for each class of input data can be explained by comparing the distribution of observed surface reflectances with values from LUT (retrieval domain). The RI is expected to be high for pixels belonging to observed and simulated surface reflectances. Table 1.1 illustrates this rule: about 65% of the GL and PL pixels are located within or near the retrieval domain, but the overlap of GH and PH data with retrieval domain is less than 30%. This explains why GL and PL data result in higher values of the RI than GH and PH data. The QA in MODAGGAG product alone does not provide enough information on input quality and thus it can not assure the successful execution of the main algorithm. A temporal analysis is required to discriminate between good and poor data quality. However, there are still 45% of GL data that is not included in the retrieval domain. The future version of algorithm should extend the retrieval domain to increase the RI. Figure 1.7 illustrate the relationship between RI and δ_{SR} : RI drops from 68% to 43% when δ_{SR} increases.

	Collection 3		Good quality, low uncertainties		Good quality, high uncertainties		Poor quality, low uncertainties		Poor quality, high uncertainties	
	\cap	\cup	\cap	\cup	\cap	\cup	\cap	\cup	\cap	\cup
Collection 3	2216	2216	755	3585	485	3157	247	2641	703	7555
Good quality, low uncertainties	755	3585	2214	2214	1216	2470	704	2274	1856	6490
Good quality, high uncertainties	485	3157	1216	2470	1516	1516	529	1749	1186	6462
Poor quality, low uncertainties	247	2641	704	2274	529	1749	762	762	754	6140
Poor quality, high uncertainties	703	7555	1856	6490	1186	6462	754	6140	6122	6122

Table 1.1. Comparison of four groups of data with the collection 3 retrieval domain.

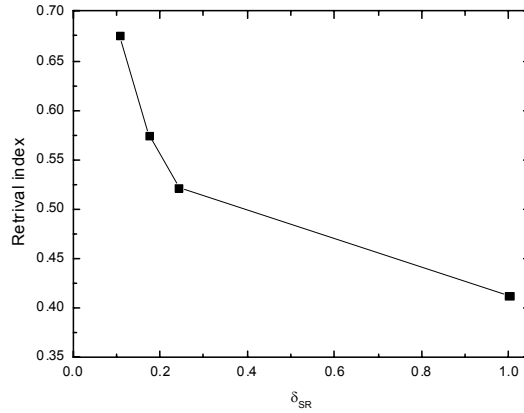


Figure 1.7: Retrieval index as a function of the uncertainties of surface reflectance

How do uncertainties in surface reflectances impact LAI retrievals? Figure 1.8a illustrates that if “good quality” data are used, the uncertainties in retrieved LAIs are about 10%. For poor quality data its value is 30%. Figure 1.8b shows the relationship between uncertainties in input and in retrievals. If uncertainties in input surface reflectance data do not exceed 20%, δ_{LAI} is nearly constant. Above this threshold δ_{LAI} increases linearly with a slope of 1.3.

(a)

(b)

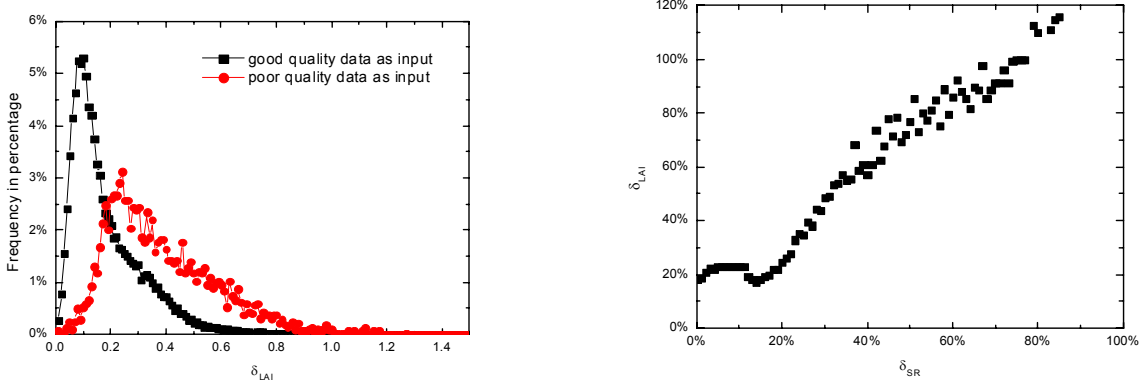


Figure 1.8: Impact of variation in surface reflectance on LAI retrievals. Panel (a) shows histograms of the coefficient of variation of LAI derived using “good quality” and “poor quality” data. Panel (b) shows variation in LAI as function of variation of surface reflectances

Conclusions

The overestimation of the MODIS LAI over Konza site is caused by two factors, namely, uncertainties in biome map and surface reflectances. The uncertainty in the MODIS LAI product can be estimated as function of biome misclassification δ_{biome} and uncertainties in surface reflectances δ_{SR} as follows:

$$\delta_{LAI} = A \times \delta_{biome} + B \times (\delta_{SR} - 15\%) + C, \text{ if } \delta_{SR} \geq 15\%,$$

$$\delta_{LAI} = A \times \delta_{biome} + C, \text{ if } \delta_{SR} \leq 15\%.$$

Here A is the coefficient that indicates the effect of biome misclassification, B is the coefficient describing the impact of uncertainties in surface reflectances, and C is a constant that represents the uncertainties in canopy radiation model used in the MODIS LAI & FPAR algorithm. It was found that A is about 0.4, $B \approx 1.2$, and $C = 0.2$. This indicates that uncertainties in LAI retrievals are limited by uncertainties in input and not uncertainties in the LAI & FPAR algorithm. To minimize the biome misclassification and uncertainties in surface reflectance, the validation of global LAI/FPAR product should be performed at a sufficiently large scale.

II. Analysis of the Performance of the MODIS LAI and FPAR Algorithm over Broadleaf Forests

Site Description

The MODIS LAI & FPAR product from the tile h12v04 was selected for this investigation. This tile contains the Harvard Forest, Petersham, MA, USA (located 42.5382° North and 72.1714° West; MODIS tile h12v04, line 895, sample 818). The site has a transition land cover dominated by mixed hardwood and conifer forests, ponds, extensive spruce and maple swamps. Harvard Forest is well known for its long history of scientific research of monitoring natural disturbances, environmental change and human impacts (WWW 6). This site was selected for several recent major field campaigns within following projects: BigFoot (WWW 1), Flux Network (FLUXNET, WWW 2), Global Landcover Test Site Initiative (GLCTS, WWW 3), Long-Term Ecological Research (LTER, WWW 4). It is also an EOS core validation site, selected to provide a focus for satellite, aircraft, and ground data collection of land product validation (WWW 5).

Data Used

- MOD15A2, 8-day LAI composite (collection 4), tile h12v04, composite 2001.001-2001.313;
- MODAGAGG, daily surface reflectance (collection 4), tile h12v04, days 2001.121-128 and 2001.193-200
- MOD12Q1, 6-biome classification map, collection 3, tile h12v04

Statement of the Problem

The evaluation of the LAI and FPAR product, collection 4, was performed for broadleaf forest at MODIS tile h12v04. The tile h12v04 contains the Harvard Forest validation site, where extensive measurements of LAI were performed recently by BigFoot and BU teams. Field measurements indicate that mean LAI is about 5.0 ± 0.85 during the summer time, while MODIS estimation is about 5.8 ± 0.9 . The discrepancy is less than 20% and is allowable by specifications of product. However, as can be seen from Figure 2.1, LAI retrievals are mainly performed by the back-up algorithm, i.e., the main algorithm failed during that period. From the other side, the main algorithm retrieves LAI without failure during spring green-up. Analysis of factors that determine such a behavior is the main objective of the research below.

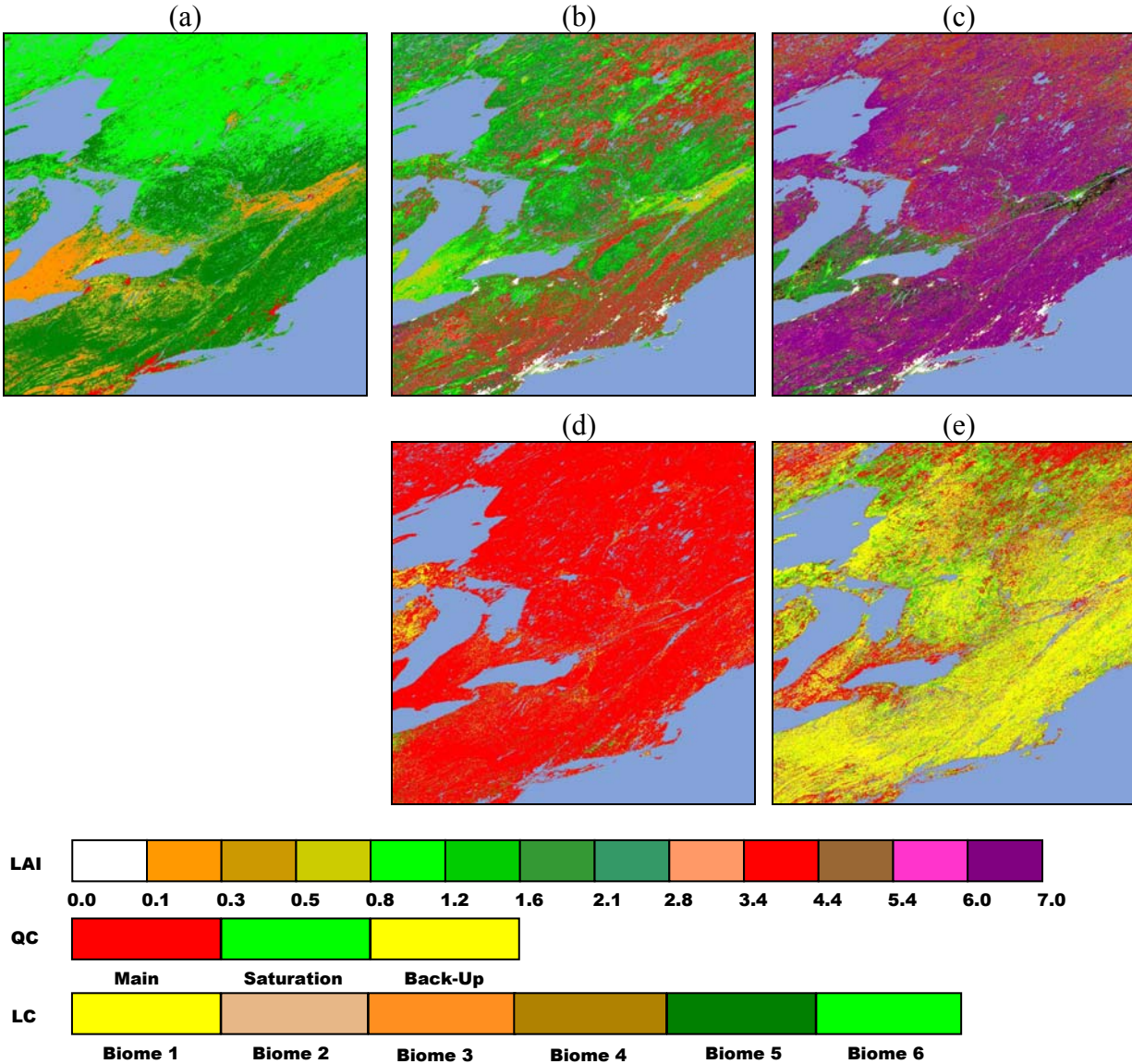


Figure 2.1: Temporal variation of the collection 4 MODIS LAI from early spring to summer for broadleaf forest in the tile h12v04. Panel (a): the 6 biome land cover map used by the collection 4 algorithm. Panel (b): LAI for May 01-08, 2001. Panel (c): LAI for July 12-19, 2001. Panel (d): QC for May 01-08, 2001. Panel (e): QC for July 12-19, 2001.

Seasonal Variations in MODIS LAI over Broadleaf Forests

MODIS LAI and FPAR product correctly captures seasonal variations in biome 5 (Broadleaf Forests) LAI. Figure 2.2a shows mean LAI and its standard deviation from MODIS collection 4 data for broadleaf forest over whole tile h12v04. During winter time and early spring (days 0-100, which is January 1 - April 10) LAI is stable and equals approximately 0.5. After short time of green-up (days 100-150, which is April 10- May 30) LAI increases up to its maximum value of about 5.8 ± 0.9 . During summer (days 150-250, which is May 30 - September 07) LAI has stable value of 5.8 ± 0.9 . After day 250 LAI is dropping down to its winter value of 0.1.

In addition to seasonal variation in LAI values, let us consider the quality of retrievals. A key indicator of the retrieval quality is the algorithm path. Three options of the execution exist and are listed in the order of decreasing quality: main algorithm without saturation, main algorithm with saturation and back-up algorithm. Figure 2.2(b) shows seasonal variations in the number of pixels generated by each of the execution branch. During the spring time green-up, the portion of pixels where LAI is produced by the main algorithm increases up to its maximum value at composite 121 (May 01-08, 2001, $LAI=2.9 \pm 1.5$) and then drops to the minimum at approximately day 153 (May 30, 2001, $LAI=5.8 \pm 0.9$). Then, during whole summer time main algorithm fails for majority of the pixels, and LAI values are generated by the back-up algorithm.

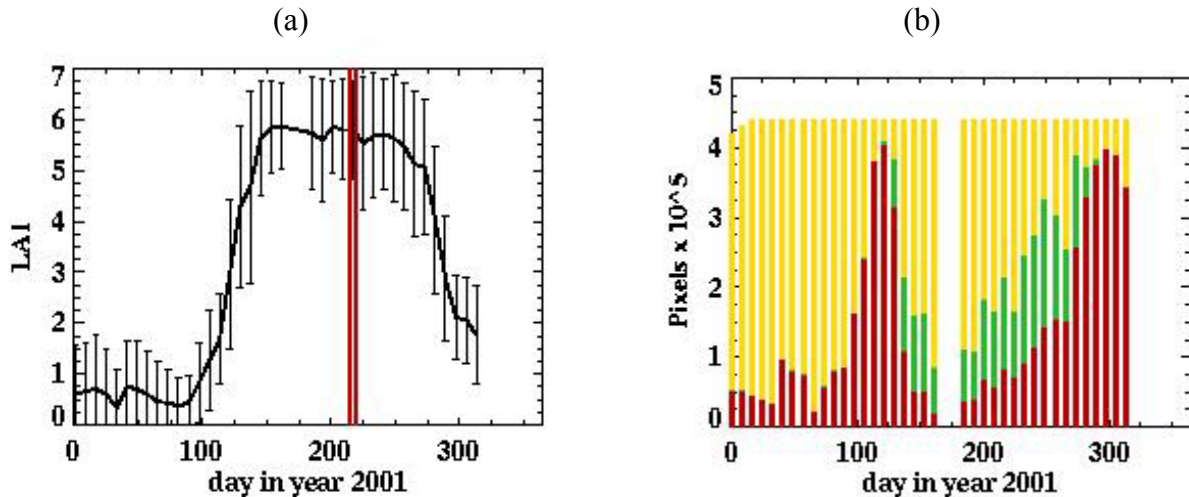


Figure 2.2. Annual variations in the collection 4 MODIS LAI retrievals over broadleaf forests for the tile h12v04. Panel (a): Mean LAI and its standard deviation. Panel (b): Number of pixels where main algorithm without saturation was executed (red), main algorithm with saturation was executed (green) and the back-up algorithm was executed (yellow). The gap in the data (days 168-185) is due to the MODIS instrument being down for that time.

Interpretation of MODIS Surface Reflectances with RT Approach

Scatter plot of the daily MODIS surface reflectances (July 19, 2001, MODAGAGG product) for broadleaf forests in the tile h12v04 is shown at Figure 2.3. Surface reflectances, processed by different branches of the algorithm are color coded for convenience of identification. Note the shape of retrieval domain for each execution branch, which presents finger print of the LUT. The main algorithm without saturation retrieves LAI for lower portion of surface reflectances. Main algorithm with saturation was executed for pixels where NIR reflectances are higher compared to the previous case. The back-up algorithm is executed when NIR is high and RED is small (small NDVI) as well as for bright patterns in both RED and NIR channels. The radiative transfer equation is used to interpret the retrieval domain of the main algorithm (for cases with and without saturation).

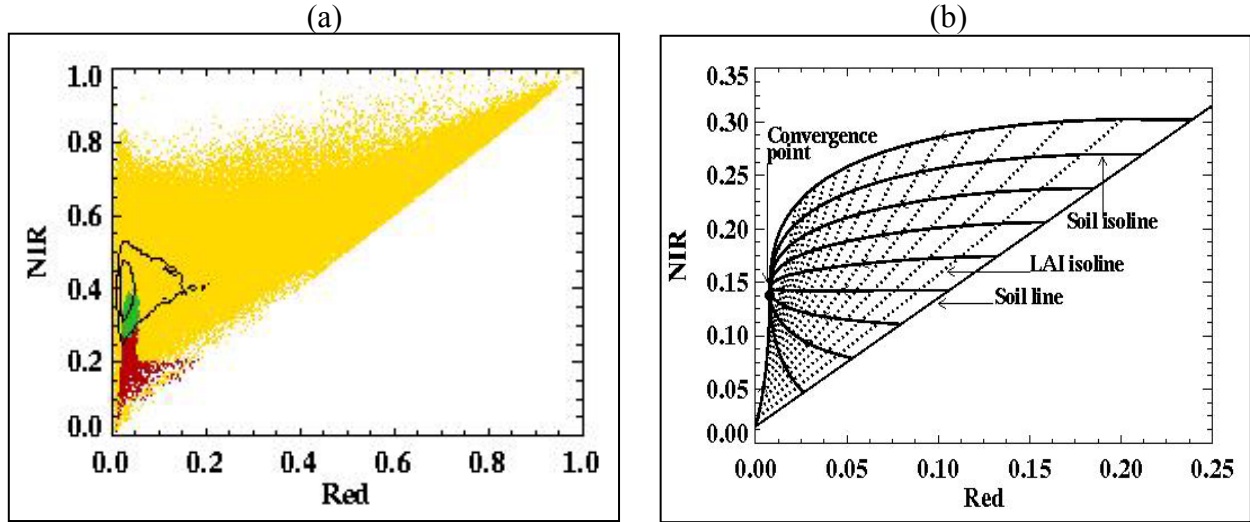


Figure 2.3. Panel (a): MODIS surface reflectances selected by different branches of the execution of the LAI and FPAR algorithm. Daily data for July 19, 2001 for broadleaf forest in tile h12v04 were used. Contours show the location of highest density data. Panel (b) shows variation in surface reflectances as a function of LAI and soil patterns. As LAI is increasing surface reflectances converge to a common point. This is a condition of saturation.

RT simulation performed with recently developed radiation model that characterizes radiative transfer in heterogeneous vegetated surfaces using stochastic concepts (Shabanov et al., 2000). To obtain a general picture of changes in the spectral space when the system (vegetation + background) is changing, it is sufficient to consider horizontally homogeneous canopy. For this purpose, leaf optical properties were assumed to be invariant and set as follows (based on average data from a spectral data bank): for grasses, $\text{refl}_{\text{red}} = 0.070$, $\text{refl}_{\text{nir}} = 0.49$; $\text{trans}_{\text{red}} = 0.030$, $\text{trans}_{\text{nir}} = 0.43$; for needle forests, $\text{refl}_{\text{red}} = 0.055$, $\text{refl}_{\text{nir}} = 0.498$; $\text{trans}_{\text{red}} = 0.040$, $\text{trans}_{\text{nir}} = 0.386$. In model calculations I used averaged optical properties of two species due to negligible effect of difference between them on model output. The initial state of the system is a bare background and is specified by background reflectance. The controlling parameter of the system is leaf area index (LAI). As LAI is increases against an invariant background, the system moves along trajectories (soil or background isolines) in the spectral space away from the initial state. To observe different trajectories, the initial conditions (background reflectances) according to the background line concept (Baret et al., 1993): $\rho_{\text{nir}}^{\text{background}} = 1.2 \cdot (\rho_{\text{red}}^{\text{background}} + 0.04)$, where $\rho_{\text{red}}^{\text{background}}$ and $\rho_{\text{nir}}^{\text{background}}$ are background reflectances at red and near-infrared wavelength were varied. The set of calculated trajectories (soil isolines) is shown in Figure. 2.3b, which also shows LAI isolines, along which LAI is constant, while the background reflectance changes (LAI change between adjacent LAI isolines is 0.25). Note that for very dark backgrounds, increasing leaf area increases both red and near-infrared reflectances, while for backgrounds of intermediate brightness, red reflectance decreases and near-infrared reflectance increases. In the case of dense canopies the trajectories converge to a common point in the spectral space, the reflectance when leaf area tends to infinity. The location of this point is determined mostly by leaf optical properties and also by canopy structural features (leaf normal orientation distribution, geometry, etc.) For example, the location of this limiting point

(hemispherical reflectances of canopy, $R^{\text{canopy}}(\lambda)$) can be analytically evaluated using a two-stream approximation (Ross, 1981) for the case of a horizontally homogeneous canopy with flat horizontal leaves,

$$\lim_{LAI \rightarrow \infty} R^{\text{canopy}}(\lambda) \rightarrow \frac{1 - \tau(\lambda) - \sqrt{(1 - \tau(\lambda))^2 - \rho^2(\lambda)}}{\rho(\lambda)},$$

where $\rho(\lambda)$, $\tau(\lambda)$ are leaf hemispherical reflectance and transmittance at wavelength λ .

Now, if we compare Figures 2.3a and 2.3b we can see that MODIS surface reflectances qualitatively follow to the patterns predicted by RT approach. Figure 2.3a also shows location of the highest density of the data in spectral space, depicted as contour plot. This contour plot only includes the best quality surface reflectances as indicated by MODAGAGG data quality control (Band_QC="Product produced at ideal quality"). Due to the fact that LAI is high for the majority of the pixels during the summer time at broadleaf forests ($LAI = 5.8 \pm 0.9$, cf. Figure 2.2) location of the highest density data should match with the limiting point at Figure 2.3b, which indicates retrievals under condition of saturation.

Comparison of MODIS LAI for Spring and Summer

To understand the reason for the failure of the main LAI algorithm in the case of broadleaf forests, let us compare its performance for the spring time, when it works for majority of the pixels. Figure 2.4 shows scatter plot of surface reflectances during May-01-08, 2001 and July 12-19, 2001, which were selected by LAI and FPAR algorithm to generate 8-days composite LAI and FPAR product. The corresponding scatter plots are overplotted with contour plots of highest data density. It follows from the comparison of Figure 2.4a and 2.4b, the reason for the main algorithm failure during summer is mismatch between domain of definition (LUTs) of the main algorithm and location in the spectral space of the highest density of surface reflectances. The algorithm is using static LUTs- the finger prints of the main algorithm LUTs for the case of main algorithm without and with saturation are exactly the same for spring and summer data. However, because of green-up, location of highest density of the surface reflectance data moved to the higher NIR (increase of 71%) and lower RED (decrease of 27.5%) location as indicated in Figure 2.4c and Table 2.1. Change of the most probable RED and NIR is accompanied with the increase of NDVI by 29.1%. Due to the fact that mean NDVI is high during the summer (NDVI=0.835) and main algorithm fails, LAI is calculated from LAI-NDVI regression curves, which also were established for lower saturation NDVI (flat part of the curve at the Figure 2.4d). Essentially the majority of LAI values are retrieved from the portion of NDVI-LAI curve where if NDVI is higher 8.5 then LAI=6.

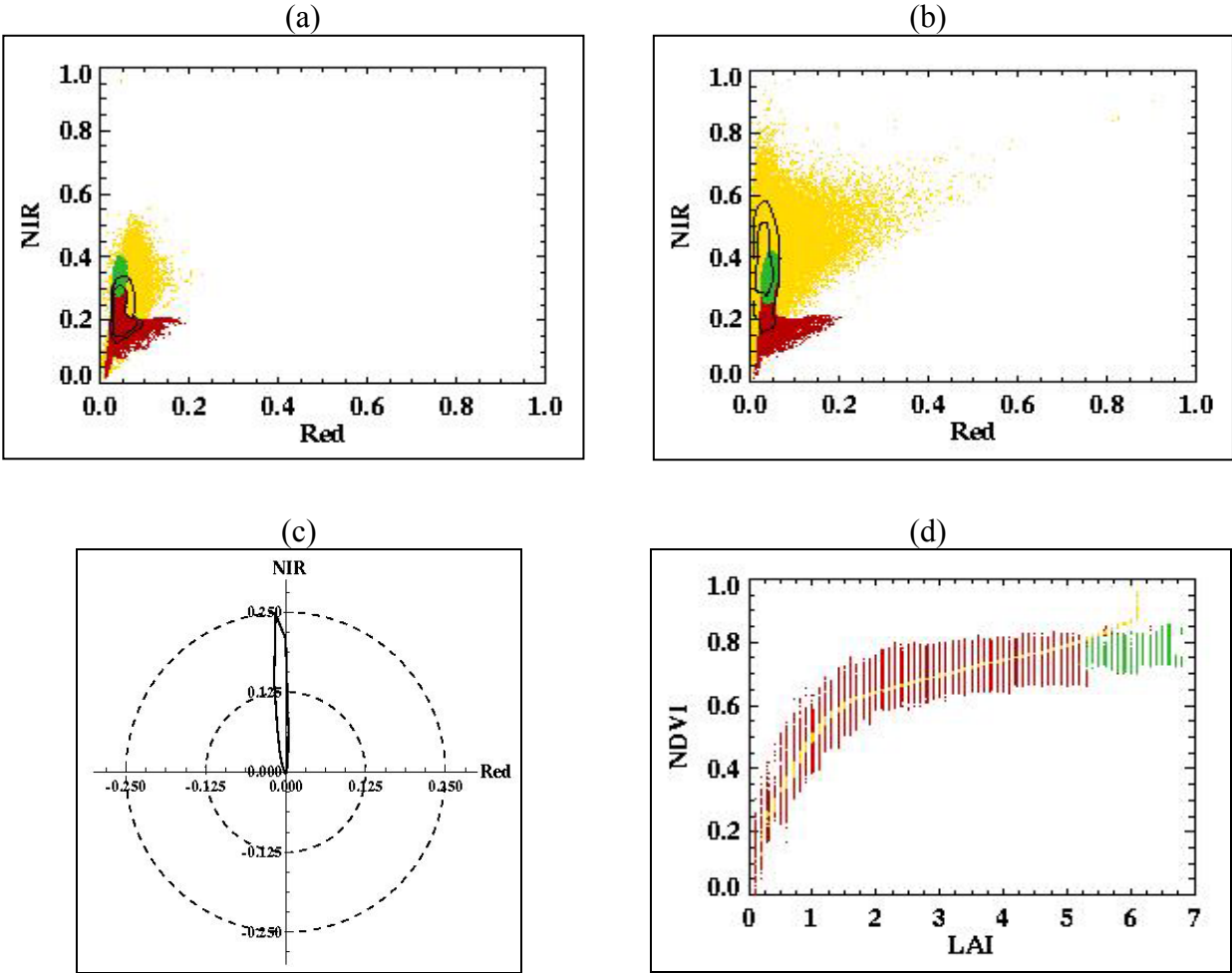


Figure 2.4. Panel (a) shows surface reflectances for May 01-8, 2001. Panel (b) shows surface reflectances for July 12-19, 2001. Panel (c) shows change of surface reflectances between the above dates. Panels (d) shows LAI-NDVI relationship established by main and back-up algorithms for July 12-19, 2001.

Variable	May 01-08, 2001	July 12-19, 2001	Change
Red	0.047	0.034	-27.5%
NIR	0.226	0.387	+71.2%
NDVI	0.646	0.835	+29.1%
LAI	2.97	5.59	+88.2%

Table 2.1: Change in surface reflectance properties for broadleaf forest at tile h12v04 during transition from spring (May 01-08, 2001) to summer (June 12-19, 2001)

Analysis of the Compositing Scheme

MODIS LAI and FPAR product (MOD15A2) is 8-day composite of daily LAI and FPAR product. In collection 4 compositing is performed using maximum FPAR over best quality retrievals (best is main algorithm without saturation, then main algorithm with saturation and the lowest level is back-up algorithm). This compositing scheme is improvement over the previously used (for collection 3 and earlier version), where maximum FPAR was done over all the daily retrievals regardless of the quality of retrievals. New compositing allows decreasing the amount of pixels in MOD15A2 product with LAI generated by back-up algorithm, due to the fact that preference in compositing is given to the best quality data, which is main algorithm without saturation. Comparing Figure 2.3a (daily data for July 19, 2001) and Figure 2.4d (8 day composite for dates July 12-19, 2001) one can note that compositing decrease amount of pixels with high RED and NIR reflectances located at soil line and compress data to the neighborhood of the domain of definition of the main algorithm. From other side, the effect of performing maximum FPAR compositing is also clear- pixels with high NDVI (and correspondingly high FPAR) beyond of the domain of definition of the main algorithm (high NIR and low RED) are inherited from daily to 8-days composite.

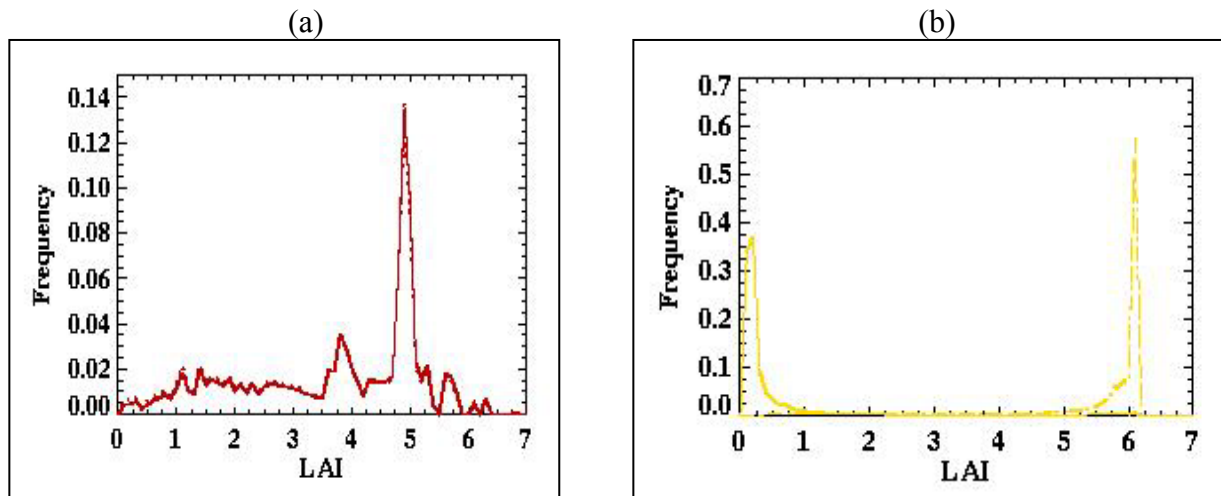


Figure 2.5: Variability of LAI during 8-days compositing period. Panel (a) shows histograms of the minimum (solid line), maximum (dashed and dotted line) and composited (dashed) LAIs for the main algorithm retrievals. Panel (b) shows the same but for back-up algorithm

Now, let us consider variability of daily LAI during 8-days compositing period, as shown at Figure 2.5. This figure shows histograms of minimum and maximum LAI during 8-days period as well as histogram of compositing LAI. There are virtually no variations between those three values for the main algorithm case. On average, only 1.1 out of 8 days for particular pixels has LAI generated by main algorithm. However, for the case of back-up algorithm, on average 7.9 days out of 8 for particular pixels have LAI generated by back-up algorithm, and boundary of variations between minimum and maximum are large (from LAI=0.5 to LAI=6). Due to the maximum FPAR compositing, always the highest LAI value is selected. This variability of LAI

retrievals generated by back-up algorithm should serve as indicator of uncertainties in surface reflectances as well as indicator of limitation of back-up algorithm on high quality retrievals.

Summary

This is an ongoing research with the goal of specifying how the parameterization of the algorithm should be improved to advance quality of the LAI and FPAR product. Key findings to the present time can be summarized as follows:

- During summertime period for broadleaf forest current LAI/FPAR algorithm does not sample in full most probable location in RED-NIR spectral space of surface reflectances. NDVI evaluated from MODIS surface reflectances is higher than what is set currently in LUTs.
- Analysis of compositing scheme indicates small variations in LAI retrieved by the main algorithm versus large variation in LAI retrieved by back-Up algorithm.

The expected changes in the algorithm will possibly include, but will not be limited to:

- Performing tuning of LUTs: leaf albedo, including more soil patterns;
- Modification to compositing scheme for Back-Up algorithm: selection of best quality input surface reflectances followed by average of LAI (not maximum FPAR).

In addition, research will be performed to assess quality of surface reflectance data. The main question is if mean value of surface reflectances (especially at NIR channel) match to the ones predicted by RT theory for vegetation canopies.

III. Maintenance of the Algorithm Issues

- Patch delivery for the TERRA LAI and FPAR algorithm to fix problem of incorrectly reading negative view azimuth angles.
- Patch delivery for the TERRA LAI and FPAR algorithm to fix problem of assigning fill value (instead of LAI=0) to pixels located at Northern high latitudes during winter time.
- Report to the MODIS landcover team about errors in latest version of MOD12Q1, 6-biome land cover product, input to MODIS AQUA and TERRA LAI/FPAR algorithm.
- Patch delivery for AQUA LAI and FPAR algorithms to update the AQUA LUT with the results of collection 4 science test for TERRA LAI and FPAR product.

IV. Future Work Plans

Current contract for development MODIS LAI and FPAR product will expire by the end of year 2003. Our team analyzed results of the research during past years and developed strategy for the future work. We submitted a proposal for NASA Research Announcement, titled "Global Products of Leaf Area Index and Fraction Vegetation Absorbed PAR from the MODIS Sensors Onboard TERRA and AQUA: EOS Algorithm Refinement Proposal". Below we summarize key points of the proposal.

Algorithm Refinement

- Evaluation of input surface reflectance uncertainties for use by the algorithm to produce LAI and FPAR fields of highest possible quality;

- Improvements to algorithm physics to account for mixture of biome architectural types within a pixel;
- Inclusion of green and blue band surface reflectances to facilitate retrievals when red and near-infrared band reflectances saturate in dense vegetation.
- Research on improvements to compositing schemes.
- Research on improvements to the back-up algorithm
- Analysis of LAI & FPAR products from Terra MODIS and Aqua MODIS

Product Analysis

- Analysis of products for spatial coverage.
- Analysis of products for accuracy
- Analysis of products for quality

QA Improvements and Operational QA of LAI & FPAR Products

- Updating QA definitions
- Inclusion of biome classification confidence level in LAI & FPAR QA
- Operational QA of the Product

Stage 2 Validation

- Achieve Stage-2 Validation for the MODIS LAI & FPAR products.
- Conduct field campaigns in collaboration with the VALERI project to facilitate assessment of product uncertainties over a widely distributed set of locations and time periods.
- Validation with data from the field campaigns and fine resolution satellite data.

Higher Resolution Products for Key FLUXNET, LBA and NACP Sites

- Generation of 250 m daily LAI & FPAR products for 50 by 50 km regions around key (core) FLUXNET, LBA and NACP sites (about 25) for 1 test year at the PI computing facility. The sites will be selected in consultation with researchers involved in these programs (the test year can be different for the three programs).
- Modifications to algorithm
- Generation of 250 m Look-Up-Tables (LUTs)
- Relations between vegetation indices and LAI & FPAR at 250 m resolution
- 250 m product generation

Comparative Investigations

- Assess the consistency between LAI & FPAR and related MODIS land products.
- Assess the consistency between LAI & FPAR products from different sensors.

Scientific Use of LAI & FPAR Products

- Global Vegetation Dynamics
- Terrestrial Carbon Cycle
- Climate Variability

Refererences

- WWW 1, BigFoot, <http://www.fsl.orst.edu/larse/bigfoot/index.html>
- WWW 2, FLUXNET, <http://daac.ornl.gov/FLUXNET/>
- WWW 3, GLSTC, <http://glcts.maxey.dri.edu/glcts/test.html>
- WWW 4, LTER, <http://lternet.edu/>
- WWW 5, EOS core validation sites, http://modis-land.gsfc.nasa.gov/val/coresite_gen.asp
- WWW 6, Harvard Forest site, <http://lternet.edu/hfr/>
- Baret, F., Jacquemoud, S., and Hanocq, J.F. (1993), The soil line concept in remote sensing. *Remote Sens. Rev.* 7: 65-82.
- Berthelot, B., Adam, S., Kergoat, L., Cabot, F., Dedieu, G., & Maisongrande, P. (1997). A global dataset of surface reflectances and vegetation indices derived from AVHRR/GVI time series for 1989 1990: The LAnd SURface Reflectances (LASUR) data. Proc. Commun. 7th Int. Symp. Physical Measurements and Signatures in Remote Sens. Courchevel, France, Apr. 7 – 11, 1997.
- Cohen, W.B., S. T. Giwer, D.P. Turner, and S.W. Running (2002), Assessment of provisional MODIS-derived surfaces related to the global carbon cycle: Land Cover, LAI, GPP/NPP, Community Outreach Workshop on MODIS Vegetation Variables Missoula, Montana, July 15- 19.
- Knyazikhin, Y., Martonchik, J. V., Myneni, R. B., Diner, D. J., and Runing, S. (1998a), Synergistic algorithm for estimating vegetation canopy leaf area index and fraction of absorbed photosynthetically active radiation from MODIS and MISR data. *J. Geophys. Res.*, 103:32257-32275.
- Knyazikhin, Y., Martonchik, J. V., Diner, D. J., Myneni, R. B., Verstraete, M., Pinty, B. and Gorbon, N. (1998b), Estimation of vegetation canopy leaf area index and fraction of absorbed photosynthetically active radiation from atmosphere-corrected MISR data. *J. Geophys. Res.*, 103:32239-32256.
- Lotsch, A., Tian, Y., Friedl, M. A., and Myneni, R. B. (2001), Land cover mapping in support of LAI/FPAR retrievals from EOS-MODOS and MISR: classification methods and sensitivities to errors. *Int. J. Remote Sens.*
- Myneni, R.B., S. Hoffman, Y. Knyazikhin, J.L. Privette, J. Glassy, Y. Tian, Y. Wang, X. Song, Y. Zhang, G.R. Smith, A. Lotsch, M. Friedl, J.T. Morisette, P. Votava, R.R. Nemani, S.W. Running (2002). Global products of vegetation leaf area and fraction absorbed PAR from year one of MODIS data. *Remote Sens. Environ.*, 83: 214-231.
- Ross, J. (1981). *The Radiation Regime and Architecture of Plant Stands*. Norwell, MA: Dr. W. Junk.
- Shabanov, N.V., Knyazikhin, Y., Baret, F., Myneni, R.B. (2000). Stochastic Modeling of Radiation Regime in Discontinuous Vegetation Canopies. *Remote Sens. Environ.*, 74(1): 125-144.
- Tian, et al., Prototyping of MODIS LAI and FPAR algorithm with LASUR and LANDSAT data, *IEEE Trans. Geosci. Remote Sensing*, 38:2387-2401, 2000.
- Wang, Y., Tian, Y., Zhang, Y., El-Saleous, N., Knyazikhin, Y., Vermote, E., & Myneni, R.B. (2001). Investigation of product accuracy as a function of input and model uncertainties: Case study with SeaWiFS and MODIS LAI/FPAR Algorithm. *Remote Sens. Environ.*, 78, 296-311.